Analyst

Accepted Manuscript

This article can be cited before page numbers have been issued, to do this please use: H. Liu, H. Yin, Y. Dong, H. Ding and X. Chu, *Analyst*, 2020, DOI: 10.1039/D0AN00156B.

View Article Online
DOI: 10.1039/D0AN00156B

Electrochemiluminescence resonance energy transfer between luminol and black phosphorus nanosheets for detection of trypsin via "off-on-off" switch mode

Hui Liu, Hao Yin, YongPing Dong*, HouCheng Ding, XiangFeng Chu*

School of Chemistry and Chemical Engineering, Anhui Province Key Laboratory of Coal Clean Conversion and High Valued Utilization, Hexian Development Institute of Chemical Industry, Anhui University of Technology, Maanshan243002, China

*Corresponding author. Tel: +86-555-2311807, E-mail address:dongyp524@163.com

View Article Online
DOI: 10.1039/D0AN00156B

Abstract

In this work, electrochemiluminescence (ECL) behavior of luminol-H_2O_2 system was studied on a black phosphorus nanosheets (BPNs) modified electrode. A quenching effect of BPNs on luminol ECL was obtained based on ECL resonance energy transfer (ECL-RET) with the excited state luminol as energy donor while BPNs as energy acceptor. Protamine could bind on the surface of BPNs through electrostatic interactions, which can cut off the energy transfer route between luminol and BPNs to restore the ECL signal. The immobilized protamine could be hydrolyzed by trypsin, as a result, the BPNs surface was exposed and the RET occurred again, resulting in the decreased ECL intensity instantly. The reduced ECL signals varied linearly with trypin concentrations, and could be indirectly used in the sensitive detection of trypsin in the range of 100 ng mL^{-1} to 5 μg mL^{-1}. The detection limit of the biosensor was calculated at levels down to 6.33×10^{-8} g mL^{-1} (3σ). The proposed ECL sensor had been successfully used in the detection of trypsin in serum samples. The results reveal novel quenching effect of BP nanomaterials on ECL, which will further expand its application in ECL biosensing for protein.

Keywords

Electrochemiluminescence, Black phosphorus nanosheets, Trypsin, Luminol, Resonance energy transfer

View Article Online
DOI: 10.1039/D0AN00156B

1. Introduction

Electrochemiluminescence (ECL) is widely used for the determination of many molecules in biology analysis due to its high sensitivity, facile manipulation, and controllable electrochemical potential.[1-3] Luminol, as a classically used organic luminophore, has outstanding advantages of low excitation potential and chemical stability.[4, 5] Reactive oxygen species (ROSs) including peroxides, superoxide radicals, hydroxyl radicals and singlet oxygen play crucial roles in the enhancement of luminol ECL.[6] So far, diverse luminol based ECL sensors have been constructed.[7, 8] For example, an ECL biosensor for glucose determination was fabricated based on quenching effect due to the consumption of dissolved O_2 via the gold nanoparticles to catalyze glucose.[9] However, such systems can only detect the H_2O_2-generating enzymes. It is still crucial to construct luminol-based ECL biosensor to detect more enzymes that do not produce hydrogen peroxide.

In the past few years, more and more layer-structured two dimensional (2D) nanomaterials, such as graphene, have become the new upstarts in ECL sensing research because of their unique and superior physical and chemical properties.[10] Since the few- and single-layer black phosphorus (BP) nanosheets were achieved in 2014 by mechanical exfoliation method, BP have triggered a recent resurgence of interest in field-effect transistors, electrocatalysis, photocatalysis, gas sensing, and so on.[11-13] However, the application of BP in electrochemical sensing still needs to be explored. Zhao and co-workers constructed an enzymatic electrochemical biosensor based on the poly-L-lysine-black phosphorus (pLL-BP) hybrid which exhibited

View Article Online
DOI: 10.1039/D0AN00156B

excellent catalytic activity toward the reduction of oxygen and hydrogen peroxide.[14] It was found in our lab that BP nanomaterials can not only catalyze electrochemical reaction of $Ru(bpy)_3^{2+}$ to generate strong anodic ECL, but also emit light in the presence of tripropylamine. Based on these findings, several ECL biosensors related to BP nanomaterials were developed.[15-17] Recently, Hu's group proposed a sensitive fluorometric method for protease detection and inhibitor screening where BPNs acted as fluorescence quencher by adsorbing the probe through electrostatic interactions.[18] However, the quenching effect of BPNs on ECL has never been reported. Thus, the new role of BPNs in ECL is still needed to be investigated.

Proteases are related closely to inflammation, emphysema, cancer, cardiovascular, viral infection, and many other physiological diseases in various physiological and pathological processes.[19] Trypsin, a typical member of the serine protease family, acts by cleaving and hydrolyzing the ester and peptide bonds involving the carboxyl groups of arginine or lysine.[20-22] Trypsin has been used increasingly for industrial applications and surgical inflammation.[23] Moreover, it has been found that the content of trypsin can be deemed as biomarkers of many important diseases.[24-26] Tremendous efforts have been made to develop convenient and effective method to realize the ultrasensitive detection of trypsin, such as mass spectrometry, colorimetric, and high-performance liquid chromatography, and electrochemical analysis.[27-30] However, high sensitive ECL method has seldom been used for trypsin determination.

In this study, a novel sensor for the detection of trypsin based on the quenching effect of BPNs on luminol ECL was designed. ECL-RET could occur between

View Article Online
DOI: 10.1039/D0AN00156B

luminol and BPNs, resulting in decreased ECL signal. Protamine (Pro) could block the RET process and restore ECL emission. When protamine was hydrolyzed by trypsin (Try), the ECL intensity decreased again. Based on this, a simple and convenient "off-on-off" mode ECL biosensor was fabricated based on BPNs, luminol, and Pro, which can be used for the detection of Try (Scheme 1).

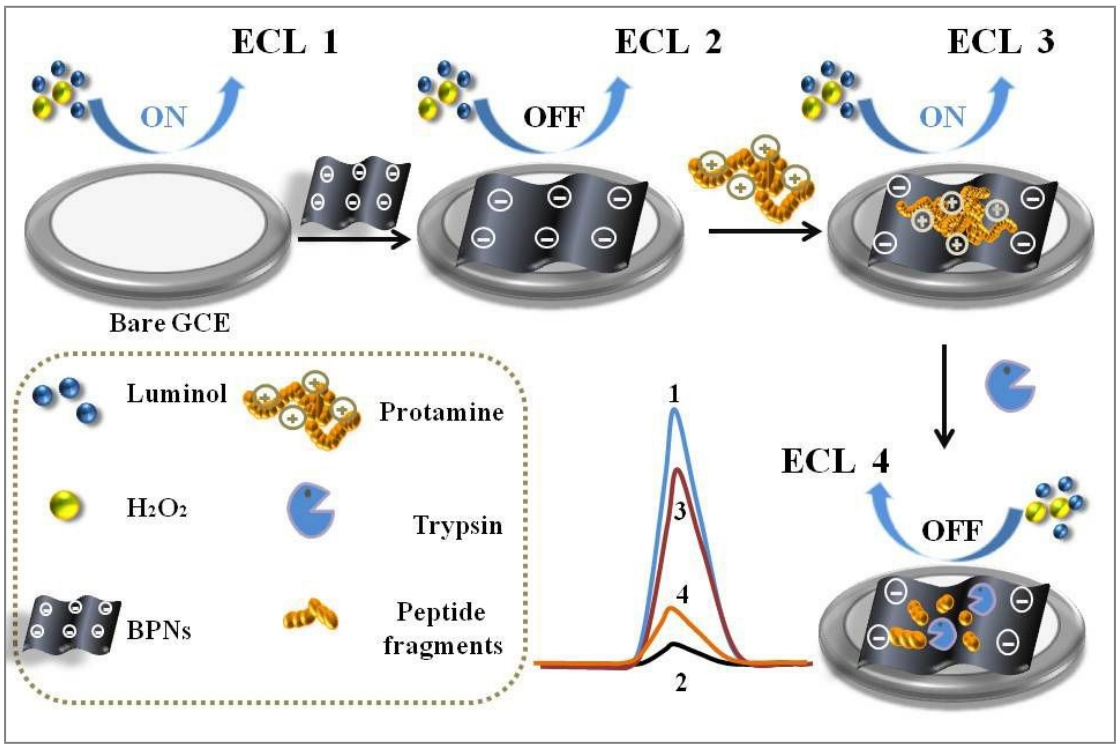

Scheme 1 Schematic illustration of the fabrication of ECL biosensor and the detection of Try.

2. Experimental

2.1. Reagents and materials

High-purity BP crystals were purchased from Nanjing XFNANO Materials Tech. Co., Ltd, China. Hydrogen peroxide was purchased from Sinopharm Chemical Reagent Co., Ltd. Luminol, glucose oxidase (GOx), bovine serum albumin (BSA) and cytochrome C (Cyt C) were obtained from Sigma-Aldrich. Protamine, lysozyme and

View Article Online
DOI: 10.1039/D0AN00156B

trypsin were purchased from Shanghai Sangon Biotechnology Company Ltd., China. 0.1 mol L^{-1} pH 7.4 phosphate buffer solution (PBS) was used to prepare the working solution. All the chemicals were of analytical grade, and were used as received without further purification. Double distilled water was used throughout. The serum samples were obtained from the First Hospital of Maanshan. All experiments were performed in accordance with the guidelines in China and approved by the ethics committee at Anhui University of Technology.

2.2. Apparatus

The ECL measurements were monitored by a model MPI-M electrochemiluminescence analyzer (Xi'An Remax Electronic Science & Technology Co. Ltd., China). The cyclic voltammetric (CV) measurement and the electrochemical impedance spectroscopy (EIS) were conducted on a CHI 760D electrochemical workstation (CH Instruments Co., China). All experiments were carried out with three-electrode system, including a modified glassy carbon electrode (GCE) as the working electrode, a platinum wire as the counter electrode and a saturated calomel electrode (SCE) as the reference electrode, respectively. The transmission electron microscopy (TEM) and high resolution transmission electron microscopy (HRTEM) was obtained on a JEOL-2100 transmission electron microscopy (JEOL, Japan). Raman spectra were collected with a Horiba JYH800 Raman spectrometer using a 532 nm laser source. Zeta potential was measured with a Zetasizer Nano ZS-90 (Malvern Instruments, Malvern, UK). FL and UV-vis absorption spectra were recorded at Shimadzu UV-3600 spectrophotometer and RF-5301PC FL

View Article Online
DOI: 10.1039/D0AN00156B

spectrophotometer, respectively.

2.3 Fabrication of ECL sensor

The synthesis method of black phosphorus is shown in the supporting information. Prior to modification, a glassy carbon electrode (GCE, 3 mm in diameter) was polished with 0.05 μm Al_2O_3 suspension to a mirror, and cleaned thoroughly in an ultrasonic cleaner with alcohol and water for 30 s, respectively. The polished GCE was further cleaned in 1 mM $K_3Fe(CN)_6$ solution between -0.20 and 0.60 V (vs SCE) at a potential scan rate of 100 mV s^{-1} until a pair of reversible peaks was obtained, indicating that the electrode surface was cleaned. After that, 10 μL of BPNs suspension was modified onto the GCE and denoted as BPNs/GCE. Next, 10 μL of 5 μg mL^{-1} protamine were spread on the BPNs/GCE for 30 min at room temperature and denoted as Pro/BPNs/GCE. Finally, the modified electrode was incubated in different concentration of trypsin (Try/Pro/BPNs/GCE) for 1 h at 37 °C. The ECL measurement was carried out at room temperature by applying the potential from -1.5 V to 1.5 V with the scanning rate of 100 mV s^{-1} in PBS with 0.01 mM luminol and 0.1 mM H_2O_2.

3. Results and discussion

3.1 Characterization of BPNs

Previous work has reported that single-layer and several layers of BPNs can be prepared by liquid-phase stripping method in organic solvents including N-methyl-2-pyrrolidone (NMP).[31, 32] In order to avoid the possible interference from organic solvent and explore the potential application of BPNs in ECL, it is necessary

View Article Online
DOI: 10.1039/D0AN00156B

to synthesize BPNs in aqueous medium. Herein, the synthesis of BPNs was accomplished by exfoliating BP crystals in water according to Wang's report.[33] The morphology of as-prepared BPNs was investigated by transmission electron microscopy (TEM). It can be found from Fig. 1A and B that BPNs show an irregular sheet-like structure. The results of HRTEM of BPNs were shown in Fig. 1C and D. Two sets of lattice fringes of 0.218 and 0.335 nm can be observed, and are assigned to the (002) and (021) plane of BP crystal, respectively. The TEM results suggest that BPNs are successfully prepared through exfoliation method in pure water. As a versatile, nondestructive method, Raman spectroscopy exhibits extraordinary advantages in characterization of various materials.[34] To figure out the structural transformation of BP during the liquid exfoliation process, the Raman spectra were measured as shown in Fig. 1E. Bulk BP and BPNs display three nearly identical peaks at 360 cm^{-1}, 437 cm^{-1} and 465 cm^{-1}, which can be assigned to the A_g^1, B_{2g} and A_g^2 of BP, respectively. These sharp patterns confirm that BPNs retain the structure of corresponding bulk counterpart.[35] Moreover, the peak location is relevant to the layer thickness according the previous literature.[14] Compared to bulk BP, three distinct peaks of BPNs exhibit a slight blue-shift, which could be ascribed to the ultrathin thickness of the nanosheets.[36] To further explore the surface charge of BPNs， Zeta potential measurement was carried out. The Zeta potential of BPNs is about −33 mV, which proves that BPNs are negatively charged (Fig. S1).

View Article Online
DOI: 10.1039/D0AN00156B

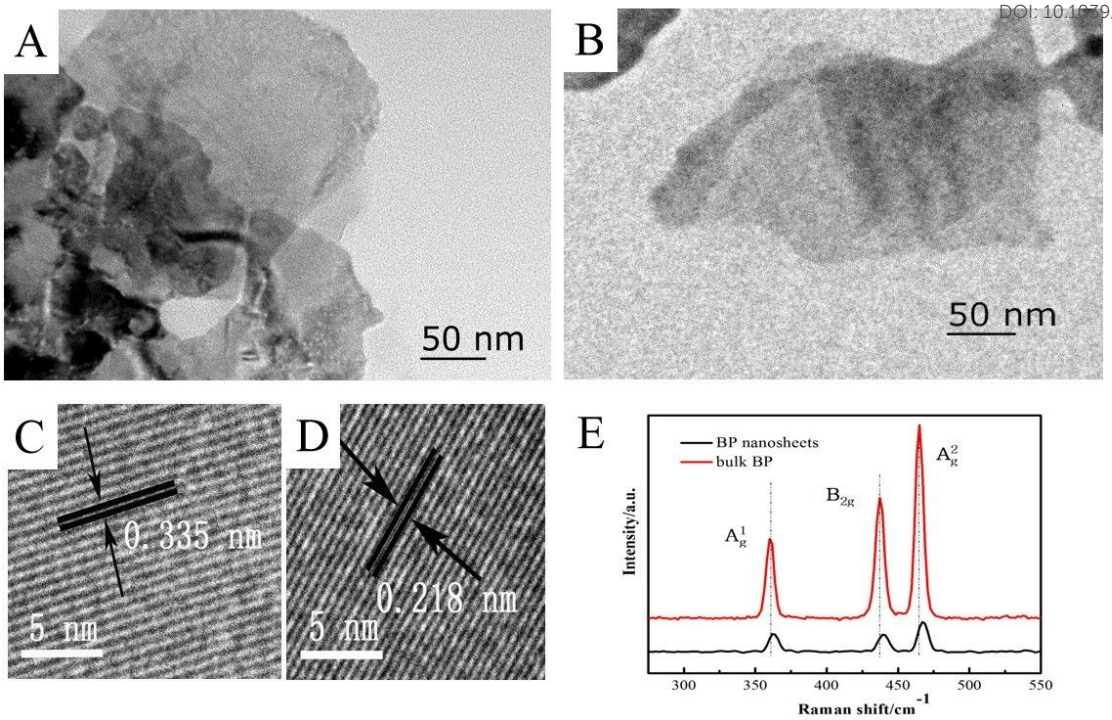

Fig. 1 (A, B) TEM and (C, D) HRTEM images of BPNs. (E) Raman spectroscopy of BPNs.

3.2 Electrochemistry and ECL of luminol at the BPNs/GCE

For exploring new role of BPNs in ECL, the synthesized BPNs were used to modify the GCE to fabricate an electrochemical platform. Luminol (LH_2) was selected as a model ECL system to explore the potential application of BPNs in the ECL field. The electrochemistry and the ECL of LH_2 were comparatively studied at a bare GCE and a BPNs/GCE in pH 7.4 PBS as shown in Fig. 2. LH_2 emits weak light under pH 7.4 condition, while the strong anodic ECL can be obtained in the presence of H_2O_2 at the bare GCE (Fig. 2A) just as reported in previous work.[37] No light emission is obtained on the BPNs/GCE in PBS solution as shown in the inset of Fig. 2A. The ECL intensity of the LH_2/H_2O_2 is significantly decreased at the BPNs/GCE, revealing the apparent inhibiting effect of BPNs on LH_2 ECL.

View Article Online
DOI: 10.1039/D0AN00156B

CV behaviors of BPNs and LH_2 were investigated in the absence and in the presence of 0.1 mM H_2O_2 at a scan rate of 100 mV s^{-1}. In LH_2 solution, one apparent oxidation peak at 0.47 V can be assigned to the oxidation of LH_2. The onset potential of LH_2 oxidation is negatively shifted and the oxidation peak current increases apparently at the BPNs/GCE compared with the bare GCE, which proved that BPNs had an obvious catalytic effect on LH_2 oxidation (Fig. 2B). Generally, the catalytic effect of nanoparticles on LH_2 oxidation will bring the stronger ECL emission.[38, 39] However, according to the ECL curve (Fig. 2A), LH_2 exhibited lower ECL signal at the BPNs/GCE than the bare electrode. It is reasonable to deduce that there might have other factor which will inhibit ECL emission. The possible reason will be discussed in the following part. The oxidation peak at 0.60 V may be assigned to the oxidation of black phosphorus itself, according to previous reports.[40]

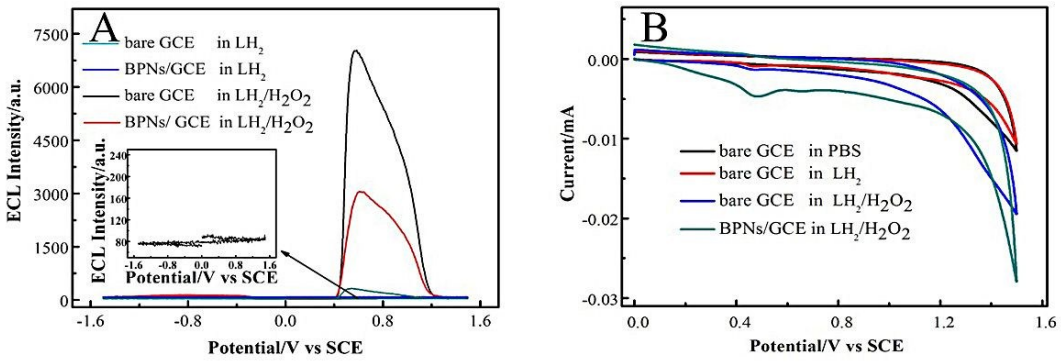

Fig. 2 ECL profiles (A) and Cyclic voltammograms (B) of different electrodes in 0.1 mol L^{-1} PBS containing 0.01 mM LH_2. Scan rate, 100 mV s^{-1}; pH 7.4.

3.3 ECL mechanisms

In order to elucidate the quenching ECL mechanism, the FL spectra of LH_2 and the mixing solution were investigated as shown in Fig.3A. The maximum FL emission

View Article Online
DOI: 10.1039/D0AN00156B

LH_2 locates at 425 nm. When LH_2 is mixed with H_2O_2, the mixture exhibits almost the same FL spectrum as that of pure LH_2. When BPNs are mixed with LH_2, the FL intensity decreases, which prove that BPNs might receive energy from the excited state of LH_2 (Fig.3A). In order to support the above speculation, the absorption spectrum of BPNs was recorded as shown in Fig.3B. The overlap between the absorption spectrum of BPNs and the FL spectrum of LH_2 suggests that the FL resonance energy transfer (FL-RET) can occur between LH_2 and BPNs. Fig. 2A revealed that the strong LH_2 ECL can be observed at the bare GCE in the presence of H_2O_2, which decreases apparently at the BPNs/GCE. The UV–vis absorption spectra of LH_2 are hardly changed with or without hydrogen peroxide and BPNs (Fig.S2), revealing that LH_2 can not directly react with hydrogen peroxide and BPNs. The CV results proved that BPNs had an obvious catalytic effect on LH_2 oxidation, which should enhance LH_2 ECL. On the contrary, LH_2 ECL was apparently inhibited at the BPNs/GCE. The inset of Fig.3B reveals the ECL spectrum is almost the same as that of FL, suggesting that ECL-RET can also occur between LH_2 and BPNs.[41] Therefore, it is reasonable to speculate that BPNs had both catalytic and quenching effects on LH_2, and these two effects can compete with each other. The variation of ECL intensity depended on the competition of these two effects. Therefore, the ECL mechanisms can be obtained according to the literature and the experimental results as follows:[6, 41]

$$\mathbf{LH^{-} - e^{-} \rightarrow L^{\bullet -}} \qquad \mathbf{(1)}$$

$$\mathbf{L^{\bullet -} + H_2O_2 \rightarrow HO_2^{\bullet} + LH^{-}} \qquad \mathbf{(2)}$$

View Article Online
DOI: 10.1039/D0AN00156B

$$HO_2^{\bullet} + OH^- \rightarrow O_2^{\bullet -} + H_2O \quad (3)$$

$$L^{\bullet -} + O_2^{\bullet -} \rightarrow AP^{2-*} \quad (4)$$

$$AP^{2-*} \rightarrow AP^{2-} + h\nu \quad \text{strong emission} \quad (5)$$

In the presence of BPNs, ECL-RET can occur between the excited state of LH_2 (AP^{2-*}) and BPNs, resulting in the inhibited ECL signal.

$$AP^{2-*} + BPNs \rightarrow \text{weak emission} \quad (6)$$

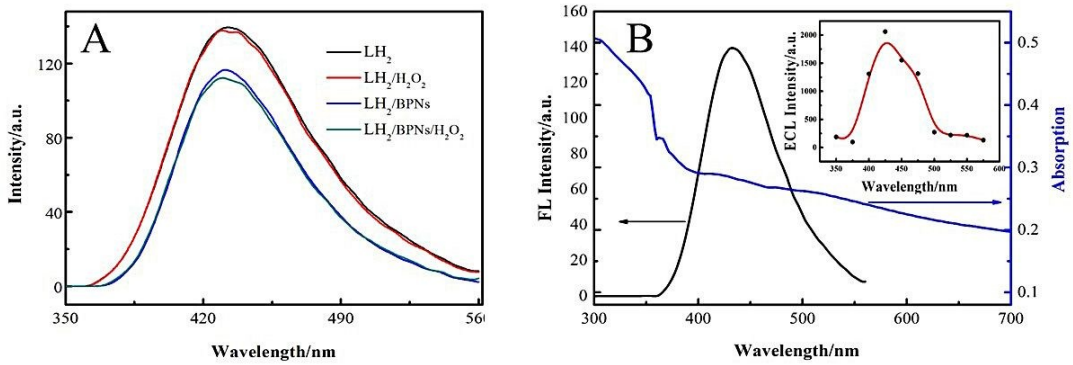

Fig. 3 (A) The FL spectra of LH_2, LH_2/H_2O_2, LH_2/BPNs and LH_2/BPNs/H_2O_2 mixing solutions. (B) The overlap between FL spectrum of LH_2 and UV–vis absorption spectrum of BPNs. The inset is the ECL spectrum of LH_2.

3.4 Fabrication of ECL biosensor

The protocol for the fabrication of ECL biosensor was shown in Scheme 1. Firstly, LH_2 was added into the solution to generate strong initial ECL in the presence of H_2O_2. Then, a "switch-off" state could be obtained by immobilizing BPNs on a bare GCE to get a quenching effect on ECL. Positively charged protamine was connected at the BPNs surface (Pro/BPNs/GCE) through the electrostatic adsorption and a "switch-on" state could be achieved. Finally, the electrode was incubated with trypsin (Try/Pro/BPNs/GCE), the "switch-off" state could be obtained again. Thus, a simple

View Article Online
DOI: 10.1039/D0AN00156B

and novel enzyme sensing platform has been established based on the relationship between the degree of peak drop and the concentration of Try.

In order to support the above strategy, the ECL responses of the modified electrodes under different stages were recorded. Strong cathodic ECL can be obtained at the bare GCE in the LH_2 solution in the presence of H_2O_2. When BPNs was modified on the bare GCE, the intensity of ECL decreased since BPNs act as an ECL energy acceptor. When protamine was modified on the BPNs film, the energy transfer route between BPNs and LH_2 was broken, which in turn causes the recovery of ECL intensity. However, owing to the partial hydrolysis of protamine by trypsin, the BP surface was exposed and the RET process occurred again. Such step can result in the reduced ECL intensity instantly again (Fig. 4A). The variation of ECL intensities can be indirectly used in the sensitive detection of trypsin.

Electrochemical impedance spectroscopy (EIS) was used to further characterize the fabrication process of the ECL biosensor as shown in Fig.4B. The equivalent circuit was used to fit the EIS data (The inset of Fig.4B). The R_{ct} for the bare GCE is 105 Ω. When BPNs were modified on the bare GCE, the R_{ct} increases to 140 Ω due to the electrostatic repulsion between the negatively charged BPNs and the $Fe(CN)_6^{3-/4-}$, indicating that black phosphorus was successfully assembled on the surface of the electrode. When protamine was modified on the BPNs film, the R_{ct} decreases to 35 Ω due to the positively charged protamine.[42] It was demonstrated that protamine successfully covered the surface of black phosphorus. The R_{ct} increases again when the electrode was incubated with trypsin, suggesting that the protamine was indeed

View Article Online
DOI: 10.1039/D0AN00156B

hydrolyzed by trypsin. The results of EIS support the successful stepwise fabrication of the ECL biosensor.

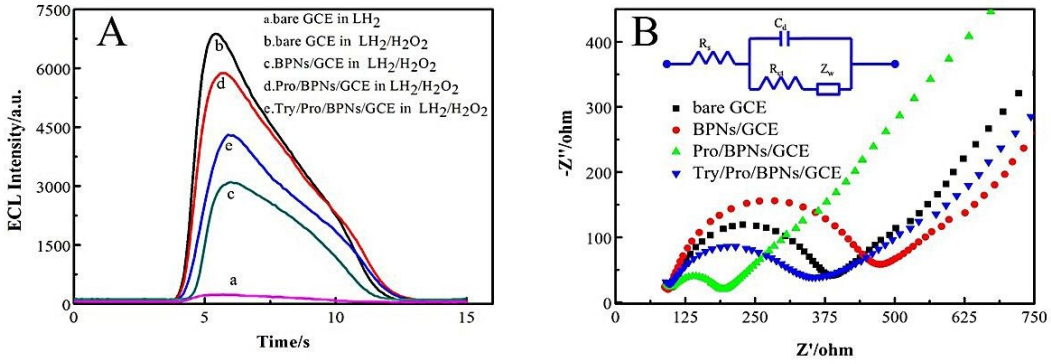

Fig. 4 (A) ECL profiles of different processes of the fabrication of biosensor. (B) Nyquist diagram of electrochemical impedance spectra recorded from 0.01 to 10^5 Hz for $[Fe(CN)6]^{3-/4-}$ (5 m M, 1:1) in 0.1 mol L^{-1} pH 7.4 PBS containing 0.1 mol L^{-1} KCl. The inset is the equivalent circuit for EIS.

3.5 Optimization of detection condition

In order to achieve the optimal performance for the detection of trypsin, several impacting factors of ECL (the pH value, the modification amount of BPNs, the concentration of protamine, and the incubation time in trypsin) were investigated (Fig. S3). The results reveal that quenching effect of BPNs increases with the increase of the modified amount of BPNs. However, the excess amount of suspension will overflow from the working area of electrode, leading to the decrease of quenching effect. Therefore, 10 μL suspension was selected. The ECL signals increase with the increase of pH values from 6.0 to 8.0 because alkaline condition is facile for LH_2 ECL. In order to fabricate biosensor in physiological condition, pH 7.4 PBS was selected as the buffer in the subsequent experiment. The ECL signals increase with the increase

View Article Online
DOI: 10.1039/D0AN00156B

of protamine concentration, suggesting that protamine have impacted the ECL reactions. In order to obtain necessary sensitivity, 5.0×10^{-6} g mL^{-1} protamine was used in the following experiment. The ECL signals decrease with the increase of incubation time of Pro/BPNs/GCE in trypsin, indicating that peptide fragments were formed owing to the hydrolysis. When the incubation time is over 60 min, the ECL signals begin to level off. As a result, 60 min was selected as the incubation time.

3.6 Analytical performance of the biosensor

In order to evaluate the quantitative behavior of the proposed ECL biosensor for the trypsin, the ECL intensity was measured through incubating the biosensor in different concentrations of trypsin as shown in Fig. 5A. It can be found that the ECL intensity decreases gradually with the increase of trypsin concentration. The inset of Fig. 5A is the 9-cycles continuous determination of 1 μg mL^{-1} trypsin using the proposed sensor. The sensor exhibits satisfactory stability with a relative standard deviation (RSD) of 1.01 %. The stable ECL signals suggest that the biosensor is suitable for trypsin detection. The calibration curve reveals a good linear relationship between the ECL intensity and the logarithm of trypsin concentration in the range from 100 ng mL^{-1} to 5 μg mL^{-1} (Fig. 5B). The linear regression equation is determined as $\Delta I= 11660.25+1619.75 \log C$ with the correlation coefficient of 0.9969. The detection limit of the biosensor is calculated at levels down to 6.33×10^{-8} g mL^{-1} (3σ, n=6). The reproducibility of the proposed biosensor for trypsin was evaluated from the response to 1 μg mL^{-1} trypsin at six different electrodes, the relative standard derivation (RSD) was 1.11 %, demonstrating that the biosensor possesses acceptable reproducibility

View Article Online
DOI: 10.1039/D0AN00156B

(Fig. 5C). In order to investigate the specific response of the biosensor to trypsin, the same experiments process were performed with 5 μg mL^{-1} bovine serum albumin (BSA), cytochrome C (Cyt C), lysozyme (Lyz), glucose oxidase (GOx), and the mixture of trypsin with them. Only the sample and the mixture of trypsin can significant decrease ECL intensity. BSA, Cyt C, Lyz, and GOx have almost negligible interference for trypsin detection (Fig. 5D). These results indicate the high specificity of the proposed sensor to trypsin.

In order to verify the practical application of the biosensor, the spike recovery method was used to evaluate the biosensor. Human serum was provided by Maanshan People's Hospital, and was diluted to 100-fold by using a PBS solution before detection. Different concentrations of trypsin (0.5, 1, 2 μg mL^{-1}) were spiked in the Human serum dilution. As seen from Table 1, the method have good spike recoveries of trypsin in the range of 96 % - 107 %, which indicates the applicable of proposed sensor in real sample detection.

View Article Online
DOI: 10.1039/D0AN00156B

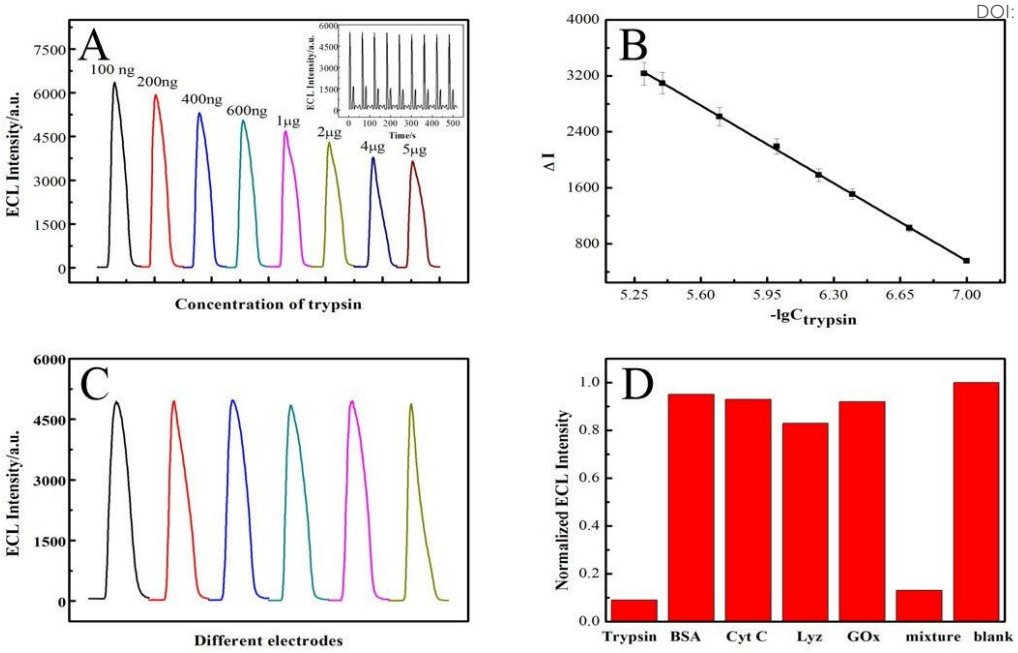

Fig. 5 (A) ECL signals of the Pro/BPNs/GCE incubated with different concentration of trypsin (from 100 ng mL^{-1} to 5 μg mL^{-1}). The inset is the stability of the sensor in 1 μg mL^{-1} trypsin under 9-cycles continuous potential scan. (B) Negative logarithmic calibration curve between ECL intensity attenuation and trypsin concentration. (C) Reproducibility of six sensors for the determination of 1 μg mL^{-1} trypsin. (D) Selectivity of the sensor to trypsin compared to possible interfering proteins: BSA, Cyt C, Lyz, GOx at 5 μg mL^{-1}, respectively.

In order to better evaluate the performance of biosensor, we compare the methods of the predecessors to those of us. As can be seen from Table S1, the analytical performance of the proposed sensor is comparable to previous reported methods. As there are very few examples of using ECL methods to detect trypsin, we hope that the present biosensor can extend the application of BP nanomaterials involved ECL system in the detection of protein.

View Article Online
DOI: 10.1039/D0AN00156B

Table 1. Detection of trypsin in human serum samples (n = 3).

Samples	Spiked(μg mL^{-1})	Found(μg mL^{-1})	Recovery (%)
1	0.5	0.48	96
2	1	1.07	107
3	2	1.93	96

4. Conclusion

In summary, anodic ECL of LH_2/H_2O_2 can be significantly inhibited on the BPNs modified electrode in neutral aqueous solution. As a result, a novel ECL resonance energy transfer system was established with LH_2 as energy donor while BPNs as energy acceptor. An "off-on-off" ECL biosensor was constructed based on the introduction of protamine on BPNs surface to impede the ECL-RET process, resulting in the variation of ECL intensity. Hence, this novel biosensor can be used in the sensitive detection of trypsin in the range of 100 ng mL^{-1} to 5 μg mL^{-1} with the detection limit of 6.33×10^{-8} g mL^{-1} (3σ). As BPNs exhibit a new role in the ECL field, we hope that more BP nanomaterials can be used in the construction of novel biosensors based on ECL-RET process.

Supporting Information

The preparation of BPNs, Zeta potential of BPNs, UV–vis absorption spectrum, optimization of detection condition and comparison of different methods for determination of trypsin are provided as Supporting Information.

View Article Online
DOI: 10.1039/D0AN00156B

Declaration of competing interest

The authors declare no competing financial interest.

Acknowledgments

This work is financially supported by National Natural Science Foundation of China (Nos.21575002, 61671019). Natural Science Foundation from the Bureau of Education of Anhui Province (Nos. KJ2019A0073, KJ2019A0052).

References

1. P. Zhao, L. F. Zhou, Z. Nie, X. H. Xu, W. Li, Y. Huang, K. Y. He and S. Z. Yao, *Anal. Chem.*, 2013, **85**, 6279-6286.

2. J. J. Ge, Y. Zhao, C. L. Li and G. F. Jie, *Anal. Chem.*, 2019, **91**, 3546-3554.

3. X. F. Tang, D. Zhao, J. C. He, F. W. Li, J. X. Peng and M. N. Zhang, *Anal. Chem.*, 2013, **85**, 1711-1718.

4. W. L. Gu, X. Deng, X. X. Gu, X. F. Jia, B. H. Lou, X. W. Zhang, J. Li and E. K. Wang, *Anal. Chem.*, 2015, **87**, 1876-1881.

5. N. Hao, X. Zhang, Z. Zhou, R. Hua, Y. Zhang, Q. Liu, J. Qian, H. N. Li and K. Wang, *Biosens. Bioelectron.*, 2017, **97**, 377-383.

6. X. J. Li, X. Sun, D. W. Fan, T. Yan, R. Feng, H. Wang, D. Wu and Q. Wei, *Biosens. Bioelectron.*, 2019, **142**, 111551.

7. M. J. Chaichi and M. Ehsani, *Sens. Actuators, B*, 2016, **223**, 713-722.

8. D. J. Li, S. S. Zhang, X., H. J. Yang, F. Nie and W. Y. Zhang, *Sens. Actuators, B,* 2019, **296**, 126631.

9. L. L. Liu, Q. Ma, Y. Li, Z. P. Liu and X. G. Su, *Biosens. Bioelectron.*, 2015, **63**, 519-524.

10. C. Z. Zhu, D. Du and Y. H. Lin, *Biosens. Bioelectron.*, 2017, **89**, 43-55.

11. H. Liu, A. T. Neal, Z. Zhu, Z. Luo, X. F. Xu, D. Tománek and P. D. Ye, *ACS Nano*, 2014, **8**, 4033-4041.

12. S. Y. Cho, Y. H. Lee, H. J. Koh, H. Jung, J. S. Kim, H. W. Yoo, J. H. Kim and H. T. Jung, *Adv. Mater.*, 2016, **28**, 7020-7028.

13. T. Sakthivel, X. Y. Huang, Y. C. Wu and S. Rtimi, *Chem. Eng. J.*, 2020, **379**, 122297.

14. Y. Zhao, Y. H. Zhang, Z. Zhuge, Y. H. Tang, J. W. Tao and Y. Chen, *Anal. Chem.*, 2018, **90**, 3149-3155.

15. L. Zhang, K. J. Tian, Y. P. Dong, H. C. Ding and C. M. Wang, *Analyst*, 2017, **143**, 304-310.

16. H. C. Ding, Z. R. Tang, L. Zhang and Y. P. Dong, *Analyst*, 2019, **144**, 1326-1333.

17. H. Liu, Y. Zhang, Y. P. Dong and X. F. Chu, *Talanta*, 2019, **199**, 507-512.

18. Z. Z. Hu, Y. X. Li, E. Hussain, X. N. Huang, Y. Y. Zhang, N. Niu, S. A. Shahzad and C. Yu, *Talanta*, 2019, **197**, 270-276.

19. C. S. Craik, M. J. Page and E. L. Madison, *Biochem. J.*, 2011, **435**, 1-16.

20. A. Bougatef, *J. Cleaner Prod.*, 2013, **57**, 257-265.

21. X. Y. Lin, Z. M. Zhu, C. F. Zhao, S. G. Li, Q. C. Liu, A. L. Liu, L. Q. Lin and X. H. Lin, *Sens. Actuators, B*, 2019, **284**, 346-353.

22. S. Y. Zhang, C. Chen, X. F. Qin, Q. C. Zhang, J. H. Liu, J. X. Zhu, Y. Q. Gao, L. Li and W. Huang, *Talanta*, 2018, **189**, 92-99.

23. N. A. Karaseva, B. Pluhar, E. A. Beliaeva, T. N. Ermolaeva and B. Mizaikoff, *Sens. Actuators, B,* 2019, **280**, 272-279.

24. J. J. Xu, E. Prost, K. Haupt and B. Tse Sum Bui, *Sens. Actuators, B,* 2018, **258**, 10-17.

25. D. Sato, T. Kondo and T. Kato, *Bioorg. Med. Chem.*, 2018, **26**, 3468-3473.

26. F. F. Xue, F. Qu, W. L. Han, L. Xia and J. M. You, *Anal. Chim. Acta*, 2019, **1046**, 170-178.

27. U. S. Lathia, O. Ornatsky, V. Baranov and M. Nitz, *Anal. Biochem.*, 2010, **398**, 93-98.

28. W. X. Xue, G. X. Zhang and D. Q. Zhang, *Analyst*, 2011, **136**, 3136-3141.

29. D. Awotwe-Otoo, C. Agarabi, P. J. Faustino, M. J. Habib, S. Lee, M. A. Khan and R. B. Shah, *J. Pharm. Biomed. Anal.*, 2012, **62**, 61-67.

30. M. Cheng, J. Zhou, X. M. Zhou and D. Xing, *Sens. Actuators, B*, 2018, **262**, 516-521.

31. X. Zhang, H. M. Xie, Z. D. Liu, C. L. Tan, Z. M. Luo, H. Li, J. D. Lin, L. Q. Sun, W. Chen, Z. C. Xu, L. H. Xie, W. Huang and H. Zhang, *Angew. Chem., Int. Ed. Engl.*, 2015, **54**, 3653-3657.

32. Z. N. Guo, H. Zhang, S. B. Lu, Z. T. Wang, S. Y. Tang, J. D. Shao, Z. B. Sun, H. N. Xie, H. Y. Wang, X. F. Yu and P. K. Chu, *Adv. Funct. Mater.*, 2015, **25**, 6996-7002.

33. H. Wang, X. Z. Yang, W. Shao, S. C. Chen, J. F. Xie, X. D. Zhang, J. Wang and Y. Xie, *J. Am. Chem. Soc.*, 2015, **137**, 11376-11382.

34. Y. Y. Li, Z. X. Hu, S. H. Lin, S. K. Lai, W. Ji and S. P. Lau, *Adv. Funct. Mater.*, 2017, **27**,1600986.

35. Y. T. Zhao, H. Y. Wang, H. Huang, Q. L. Xiao, Y. H. Xu, Z. N. Guo, H. H. Xie, J. D. Shao, Z. B. Sun, W. J. Han, X. F. Yu, P. H. Li and P. K. Chu, *Angew. Chem., Int. Ed. Engl.,* 2016, **55**, 5003-5007.

36. Z. B. Sun, H. H. Xie, S. Y. Tang, X. F. Yu, Z. N. Guo, J. D. Shao, H. Zhang, H. Huang, H. Y. Wang and P. K. Chu, *Angew. Chem., Int. Ed. Engl.,* 2015, **54**, 11526-11530.

37. Z. Zhang, J. H. Lai, K. S. Wu, X. C. Huang, S. Guo, L. L. Zhang and J. Liu, *Talanta*, 2018, **180**, 260-270.

38. H. Ke, X. Zhang, C. S. Huang and N. Q. Jia, *Biosens. Bioelectron.*, 2018, **103**, 62-68.

39. S. K. Li, Z. T. Liu, J. Y. Li, A. Y. Chen, Y. Q. Chai, R. Yuan and Y. Zhuo, *ACS Appl. Mater. Interfaces*, 2018, **10**, 14483-14490.

40. L. Wang, Z. Sofer and M. Pumera, *ChemElectroChem*, 2015, **2**, 324-327.

41. Y. P. Dong, J. Wang, Y. Peng and J. J. Zhu, *Biosens. Bioelectron.*, 2017, **94**, 530-535.

42. Y. X. Gao, K. L. Wei, J. Z. Li, Y. Li and J. Hu, *Sens. Actuators, B*, 2018, **277**, 408-414.